COMPARISON OF GAS-CONDENSATE RELATIVE PERMEABILITY USING LIVE FLUID vs. MODEL FLUIDS

N. R. Nagarajan, M. M. Honarpour, K. Sampath
ExxonMobil Upstream Research Company, Houston, USA
D. McMichael
ExxonMobil Production Company, Houston, USA

This paper was prepared for presentation at the International Symposium of the Society of Core Analysts held in Abu Dhabi, UAE, 5-9 October, 2004

ABSTRACT

Reliable predictions of well deliverability and liquid recovery from a gas-condensate reservoir require an accurate knowledge of the flow characteristics of the gas and liquid (condensate) phases through reservoir rocks. The relative permeability of flowing phases is significantly impacted by liquid accumulation in the pore space below the fluid dew point pressure and by the initial water saturation in the reservoir rock It is general practice in the industry to conduct laboratory flow tests in reservoir core plugs using synthetic (model) fluids at moderately low laboratory pressures and temperatures and to use the results for reservoir condition flow calculations. Even though the model fluid properties are adjusted to closely reflect the reservoir fluid, the model fluid does not always accurately capture the flow characteristics of compositionally complex reservoir fluid and in particular, may not mimic the reservoir wettability. This leads to significant uncertainties while using model fluid results in reservoir simulation and well deliverability calculations.

Recently, we have designed, constructed, and commissioned a unique apparatus to measure gas-condensate relative permeability at reservoir conditions using live reservoir fluids. The apparatus is capable of acquiring data at pore pressures up to 10,000 psi (at confining pressures up to 15,000 psi) and temperatures up to 250 °F. The liquid saturation is measured by a combination of chromatography and image analysis of the liquid meniscus in the separator. A steady-state method was employed for the measurements in both carbonates and sandstones with and without initial water saturation. Three model fluids and two live reservoir fluids were used in these measurements. The reservoir fluid results differ significantly from the model fluid results indicating lower gas and condensate relative permeability compared to model fluid tests. We believe that the live fluid data closely represent the reservoir condition flow and should therefore be used in all reservoir flow calculations. The results of flow tests in the presence of initial water saturation suggest that the gas relative permeability is a function of total liquid saturation and the condensate relative permeability improves in the presence of initial water saturation.

INTRODUCTION

Gas-condensate fields constitute a majority of gas reservoir assets worldwide and have become a major focus of the energy industry recently. Efficient and cost-effective reservoir management of gas-condensate fields requires meeting the unique production challenges posed by these assets, such as accurate well deliverability and liquid recovery predictions[1,2]. For example, the well deliverability and liquid recovery dictate the number of wells and the size of the surface facilities required. Fundamental to reliable predictions of well deliverability and liquid recovery over the life of the reservoir is a clear understanding and accurate knowledge of the flow characteristics[3] of both gas and condensate phases through reservoir rocks.

The flow behavior of gas-condensate fluids through reservoir rocks is an imbibition process (increasing liquid saturation) that exhibits unique characteristics different from a drainage gas-oil (decreasing liquid saturation) process[4]. Thus, the knowledge derived from conventional gas-oil displacement behavior does not necessarily extend to gas-condensate reservoirs. In particular, the gas flow in near-wellbore regions of a gas-condensate reservoir is significantly affected by the liquid accumulation[5] around the wellbore, where larger pressure drop and higher gas flux are encountered. Figure 1 shows a plot of productivity index as a function of reservoir pressure for a typical well in a lean gas-condensate[1] reservoir. A significant drop in well productivity was encountered as the flowing bottom hole pressure declined below the fluid dew point pressure. In addition, the presence of initial water saturation[6,7] in the reservoir rock may influence the gas and condensate flow. High gas rates can also affect gas flow through inertial 'non-Darcy' effects[8]. Finally, the pore structure and lithology of reservoir rocks, such as the pore/pore throat size and pore connectivity, also influence the flow behavior of both the gas and condensate phases.

GAS-CONDENSATE FLOW CHARACTERISTICS

In this section, various flow regimes associated with gas and condensate phases below the fluid dew point pressure are briefly discussed. During the production of a gas-condensate reservoir, heavier hydrocarbon components in the gas drop out as liquid when the reservoir pressure declines below the fluid dew point pressure. Figure 2 schematically displays the various flow regions encountered in a gas-condensate reservoir, along with the pressure profile and the liquid dropout curve as the pressure declines below the dew point pressure. Farthest from the wellbore (region I in the inset of Figure 2), the reservoir may still experience a single gas-phase flow because the reservoir pressure is still above the dew point pressure.

In the region where the reservoir pressure is just below the dew point pressure (region II in the inset of Figure 2), condensation of heavier components and subsequent liquid buildup occur. If the liquid saturation has not exceeded a threshold value known as the "critical condensate saturation" (S_{cc}), the liquid does not flow. However, increasing condensate saturation, even if it is not flowing, could impede the gas flow, thus reducing the well deliverability. Further to the left of this region and closer to the wellbore (region

III in the inset of Figure 2), the condensate accumulation is accelerated due to the large influx of gas in this region. This results in liquid saturation above S_{cc} and leads to two-phase flow and further loss of well productivity. The liquid saturation in this region can build up to much higher values than S_{cc}, depending on the rate of condensate dropout and the rate of condensate flow (a function of condensate relative permeability), resulting in trapped gas saturation. Finally, in the region very close to the wellbore, the high gas velocities may initially deter condensate accumulation since the liquid droplets may be carried into the well bore as a mist. But as the liquid from region III flows into region IV, two-phase flow will occur in this region as well.

The flow rate of the gas-condensate in these regions is influenced by several factors. Some of the key parameters are the absolute permeability of the rock, the relative permeability, interfacial tension and viscosity of the flowing phases. Other competing factors [e. g., viscosity ratio between the flowing phases, the ratio of gravity to capillary forces (Bond number), the ratio of inertial to viscous forces (Reynolds number), the ratio of viscous to capillary forces (capillary number), and the rock-fluid interaction (wettability)] determine the most dominant parameters that influence fluid flow at a specific flow condition. Therefore, a laboratory program should focus on designing flow tests to study the effects of all the relevant parameters on the flow in the reservoir.

GAS-CONDENSATE FLOW MEASUREMENTS

Laboratory techniques to measure gas and condensate relative permeability, critical condensate saturation, and trapped gas saturation are reviewed briefly. Most of them are modified versions of the procedures used for gas-oil relative permeability measurements. Different techniques for flow measurements for gas-condensates such as depletion tests and steady state and pseudo steady state displacements, are discussed in the literature[9].

In a depletion method, relative permeability data are measured by a constant volume depletion (CVD) process[10] to simulate the gas-condensate flow with increasing liquid saturation. In this type of depletion test, the liquid saturation cannot exceed the maximum liquid dropout in the CVD thus limiting acquisition of data at higher liquid saturation as encountered in near-wellbore regions. Another serious issue with this method is that the interfacial tension (IFT) varies throughout the test because of changing pressure or temperature causing the condensate relative permeability to decrease with increasing liquid saturation. In the steady-state technique[11,12], equilibrium liquid and gas phases are injected simultaneously into the core and the phase relative permeability data are derived from the fractional flow rates and the pressure drop across the core. By changing liquid to gas injection ratio a range of saturation is achieved in the core. However, these tests may take several days to reach steady state condition.

The pseudo-steady-state technique, proposed by Fevang and Whitson[13], measures the gas relative permeability (k_{rg}) as a function of (k_{rg}/k_{rc}) and capillary number, where k_{rc} is the condensate relative permeability, with no saturation measurements in the core. In this method, a single-phase mixture is injected through a back-pressure regulator set at a

lower pressure to flash the mixture into liquid and gas phases before entering the core. The injected liquid and gas volumes are calculated using the mixture PVT properties. k_{rg} and (k_{rg}/k_{rc}) are then calculated using the pressure drop and the fluid viscosity.

Early gas-condensate flow tests were conducted at ambient conditions with fluids very different from the reservoir fluids such as water-gas systems and mixtures exhibiting liquid-liquid equilibrium. Recent experimental studies have used synthetic fluid mixtures of two to several pure components by closely matching reservoir fluid properties. Although attempts have been made to match the model fluid properties closely with those of live reservoir fluids, often a synthetic fluid does not adequately capture the compositionally complex reservoir fluid characteristics. More importantly, the model fluid will not accurately mimic reservoir rock-fluid interaction that has a strong influence on k_{rg}, k_{rc}, and S_{cc}. Scaling up model-fluid results to reservoir conditions in the absence of a reliable technique for in-situ saturation monitoring poses problems. When used in well deliverability calculations, inadequacies of model-fluid results will lead to significant uncertainties in predicted performance.

CURRENT RELATIVE PERMEABILITY MEASUREMENTS

Relative permeability measurements were conducted using sandstone and reservoir and outcrop carbonate cores. Flow tests were conducted by steady-state method (co-injection of equilibrium phases using three model-fluids and two actual reservoir fluids.

Apparatus

A schematic of the reservoir-condition flow apparatus is shown in Figure 3. The flow system consists of a large oven housing three 2-liter high-pressure bottles (gas, condensate, and recovery), a core holder for housing the core assembly (core composite), and a windowed cell (sight glass). Three pairs of dual-cylinder syringe pumps operating in a push-pull mode circulate the fluids at a constant rate through the core assembly or withdraw the fluids from the recovery cylinder back into the sample bottles. The windowed cell serves as a separator and is used to monitor and record the produced liquid volume. The core holder is equipped with three pressure taps to allow detection of localized liquid saturation caused by heterogeneity or capillary end effects. The fractional flow of the gas and liquid is measured using a wet gas meter and a combination of chromatography and liquid level monitoring device. The apparatus is capable of operating at pore pressures up to 10,000 psi (with confining pressures up to 15,000 psi) and temperatures up to 250°F and can accommodate core composites 1-2 feet long.

Fluids Used in the Study

Three different model fluids and two live reservoir gas-condensate fluids were used in these flow tests. The model fluids were mixtures of either a binary or a ternary system of pure components. The binary mixture was made of methane and n-butane at 1710 psig and 100 °F. The two ternary fluids were mixtures of either a methane, n-butane and n-decane (ternary hydrocarbon) or n-heptane, brine, and iso-propyl alcohol (ternary aqueous mixture). The hydrocarbon ternary system exhibited gas-condensate behavior at

175 °F. The composition of this mixtures was selected to match the viscosity and IFT to those of the actual reservoir fluids at reservoir conditions. The ternary aqueous mixture exhibited liquid-liquid equilibrium at ambient conditions that represented condensate and gas phases with proper adjustment of IFT. Table 1 displays the composition and properties of the equilibrium phases of the binary and the ternary mixtures.

The reservoir fluids were a lean and a rich gas-condensate, with a condensate gas ratio (CGR) of about 55 STB/million scf and 150 STB/million scf, respectively. The compositions of these fluids are shown in Table 2. The rich and lean fluids exhibited dew point pressures of about 6000 and 6800 psia and maximum liquid dropouts of 30% and 8%, respectively, at 235 °F. The reservoir fluids and the equilibrium phases were prepared by recombining the respective stock tank condensates with synthetic gas mixtures matching their dew point pressures. The flow tests were conducted at the reservoir temperature of 235 °F using equilibrium gas and liquid phases at 4500 psia and 5000 psia for the rich and lean gas-condensates, respectively.

Cores Used in the Study

Core plugs from both carbonate and sandstone formations including the outcrop from Cordova Cream Limestone were used in assembling core composites except for carbonate reservoir plugs. Each core composite used four to six plugs that were from the same reservoir section with similar absolute permeability values. The core plugs were 2" in diameter and about 2.5" to 3.0" in length. The plugs were screened by a CT scanner and assembled in the order determined by Huppler method[14]. The core composite was then wrapped in a lead sleeve that was squeezed in place by applying confining stress. A net confining stress of 1500 to 2000 psi was maintained. The properties of core plugs and the composites are given in Tables 3 and 4 for the sandstones and carbonates, respectively.

Experimental Procedure

A steady-state technique was employed to measure the gas and liquid relative permeability by co-injecting the equilibrium liquid and gas phases through the core. A range of liquid saturation values was achieved in the core by varying the gas to liquid injection ratios between. The injection rates ranged between 2 to 3 ccs/min giving gas velocities ranging between$1x10^{-5}$ and $2x10^{-5}$ m/s. The corresponding capillary numbers ranged between $5x\ 10^{-6}$ to $1x10^{-5}$. The average liquid saturation across the core composite was calculated by measuring the injected and produced liquid volumes and verified by material balance calculations. The relative permeability to gas and liquid phases was calculated using fractional flow and the pressure drop across the core composite. The critical condensate saturation was estimated by extrapolating the liquid relative permeability data to zero value and hence very subjective. Table 5 provides a list of all the flow tests conducted along with the fluids and core samples used.

RESULTS AND DISCUSSION

Measurements in Sandstone Cores

The ternary aqueous mixture was used in four tests, the binary gas-condensate mixture was used in one test, and actual reservoir fluids were used in all five tests (see Table 5). The interfacial tension values of both model fluids were matched to that of the lean or rich gas-condensate as appropriate. The flow tests with aqueous ternary mixture were conducted at ambient conditions and the binary mixture tests were conducted at 1710 psia and 100°F. The reservoir condition tests were conducted at 4500 psi (rich condensate) or 5000 psi (lean condensate) and at 235 °F.

The relative permeability results are shown in Figures 4 and 5 for the aqueous ternary mixture and the binary mixture, respectively. As shown in Figure 4, in liquid-liquid flow tests, the relative permeability of heptane-rich liquid phase (representing the gas phase) shows a trend of correlating with the core absolute permeability. However, the water-rich phase relative permeability (representing the condensate phase) does not show any particular trend. Since the water-rich and heptane-rich phases are characteristically different from the real reservoir fluid gas and condensate phases (except for the IFT match), an in-depth analysis of these data may not provide much insight into gas and condensate flow. As illustrated in Figure 6, displaying all model fluid results, the binary relative permeability data lies at the upper bound of the ternary results.

Two of the reservoir-condition results from sandstone flow tests are displayed in Figures 7 and 8 for a lean and a rich gas-condensate, respectively. In both of these tests, critical condensate saturation estimates have higher uncertainties as the lowest saturation data starts only at higher than 40% pore volume. The trapped gas saturation (k_{rg} end point) with lean gas-condensate is fairly low (about 10%) compared to about 25% in the case of rich gas-condensate.

Measurements in Carbonate Cores

Relative permeability measurements were conducted on outcrop limestone core composite and carbonate reservoir core plugs from reef and lagoonal facies. The outcrop limestone tests employed both a model fluid (aqueous ternary mixture) and a lean condensate reservoir fluid whereas the reservoir-core plug measurements used the ternary hydrocarbon mixture as the gas-condensate fluid.

The outcrop limestone results for the model fluid are shown in Figure 9. The flow tests were conducted with and without initial water saturation. The gas relative permeability results do not show any significant differences and they seem to be functions of total liquid saturation. However, the condensate flow curves show marked deviations increasing significantly faster with liquid saturation in cores with initial water saturation compared to dry core composites. This may be due to the differences in capillary forces experienced by the condensate in the dry versus water-wet cores.

Relative permeability data measured on reef and lagoonal facies of carbonate reservoir cores using the ternary hydrocarbon mixture are shown in Figures 10 and 11. Initial water saturation was established in both the cores by saturating them with brine and displacing brine with n-decane. The critical condensate saturation was determined by a depletion flow test in which the first condensate flow was visually observed through the sight glass. At the critical condensate saturation, the gas relative permeability drops to 0.2 for the carbonate reef facies and about 0.5 for the carbonate lagoonal facies. Note that a reliable critical condensate saturation is best obtained by a depletion technique in these cores.

Comparison of Model-Fluid and Reservoir-Fluid Results

As discussed earlier, the gas-condensate flow is controlled by a combination of gravity, capillary, and viscous forces, the dominant among these forces being determined by reservoir, the depletion strategy, and production rates. These forces, in turn, are governed by rock and fluid properties and the rock wettability. All the flow tests including those with model fluids reported here were conducted in the reservoir condition apparatus. Figure 12 displays the results of the model-fluid and reservoir-fluid tests conducted on the outcrop limestone core composites. The model fluid used was an aqueous ternary mixture described above. The reservoir fluid used was the lean gas-condensate (Table 2). At any given liquid saturation, the reservoir fluid k_{rg} is significantly lower than the model fluid k_{rg}. Although condensate relative permeability curves seem to be similar for both reservoir and model fluids, the trapped gas saturations (S_{gt}) are very different, the model fluid S_{gt} being higher than the reservoir fluid S_{gt}. The main causes for these differences may stem from the differences in rock-fluid interactions exhibited by the model and reservoir fluids.

Figure 13 displays the results of relative permeability measurements using model fluids and a rich reservoir fluid in a sandstone core composite. The model fluids used were the binary mixture and the aqueous ternary mixture. The reservoir-fluid tests indicate lower relative permeability to gas and condensate phases than those obtained from model-fluid tests. The reservoir-fluid data are likely to be more reliable and representative of reservoir flow behavior because they duplicate more accurately the fluid and rock properties and rock-fluid interactions such as wettability characteristics. Figure 14 displays the reservoir and model fluid relative permeability data shown in Figure 13 in another widely used format[13, 15], k_{rg} vs. (k_{rg}/k_{rc}) ratio. The reservoir fluid data falls below the data for both the model fluids. This indicates that for a given k_{rg}, the ratio k_{rg}/k_{rc} is higher for the reservoir fluid than the model fluid. Thus, at any given k_{rg}, k_{rc} is lower leading to further condensate build-up. This is a significant observation based on the extensive data we have measured in our laboratory. We attribute the differences between reservoir and model fluid results to several factors including difficulty in controlling phase behavior and phase stability, slight differences in matching fluid properties leading to larger differences in competing forces in play (e. g., viscosity ratio, viscous to capillary forces, etc.), and the obvious differences in wettability characteristics.

Effect of Initial Water Saturation

The results of flow tests in the presence of initial water saturation suggest that the gas relative permeability is influenced by the total liquid (water and condensate) saturation and thus the presence of immobile water does not appear to significantly impact the gas permeability. However, it is observed that the presence of initial water saturation improves the condensate relative permeability as shown in Figure 15 for reservoir fluid tests in sandstones. This may indicate that the presence of immobile water saturation in water-wet sandstone cores may promote for the condensate flow by a smooth water coating on the rock surfaces.

CONCLUSIONS AND RECOMMENDATIONS

- Complete quantification of gas-condenstate relative permeability requires a combination of depletion test for critical condensate saturation followed by a steady state test for gas-condensate relative permeabilities.
- Relative permeability data measured using live reservoir fluids at reservoir conditions differ significantly from those of model fluids. In cores we studied, both the gas and condensate relative permeability using reservoir fluids are found to be lower than those measured with model fluids at any given liquid saturation.
- It is demonstrated that at any given gas relative permeability, the condensate relative permeability is lower in the case of reservoir fluids thus possibly leading to higher condensate saturation build-up than those indicated by model fluid measurements.
- The presence of initial water saturation may not significantly impact the gas relative permeability; however, it could have significant impact on the condensate relative permeability.

Finally, we believe that reservoir-fluid data are likely to be more representative of fluid flow in the reservoir as these tests closely mimic the reservoir flow environment. It is recommended that we use relative permeability obtained using reservoir fluids in all reservoir flow calculations. Model fluids results may be used only when the validity of these results is established by comparing them with reservoir-fluid measurements.

ACKNOWLEDGEMENTS

We would like to thank the management of ExxonMobil Upstream Research Company for allowing us to publish these results. We also thank the management of ExxonMobil Production Company for allowing us to include some of their data in this article. We would also like to acknowledge R. C. Glotzbach and C. A. Crowell for performing some of the flow tests.

REFERENCES

1. Affidick, D., Kaczorowski, N. J., Bette, S., "Production Performance of a Retrograde Gas Reservoir: A case Study of the Arun Field", SPE 28479, (1994), SPE Asia Pacific Oil and Gas Conference, Melbourne, Australia.

2. Barnum, R. S., Brinkman, F. P., Richardson, T. W., and Spillette, A. G., "Gas Condensate Reservoir Behavior: Productivity and Recovery Reduction Due to Condensation", (1995) SPE 30767, SPE Annual Technical Conference and Exhibition, Dallas, TX.
3. Fevang, O. and Whitson, C. H., "Modeling Gas Condensate Well Deliverability", SPERE, (1996), 221.
4. Muskat, M.: Physical Principles of Oil Production, McGraw-Hill (1949).
5. Bourbiaux, B. J., "Parametric Studies of Gas-Condensate Reservoir Behavior During depletion: A Guide for Development Planning", SPE 28848, European Petroleum conference, (1994), London, UK.
6. Danesh A. et al, "Experimental Investigation of Critical Condensate Saturation and Its Dependence on Interstitial Water Saturation in Water-Wet Rocks", SPERE, (1991), 336 and Trans. AIME, (1991), 291.
7 Lombard, J-L, Longeron, D. and Kalaydjian, F., "Well Productivity of Gas-Condensate Fields: Influence of Connate Water and Condensate Saturation on Inertial Effects", SCA 9929, (1999), Intnl. Symposium of the Society of Core Analysts, Golden, Colorado, USA.
8. Narayanaswamy, G., Pope, G. A., Sharma, M., M., Huang, M. K., Vaidya, R. N., " Predicting Gas-Condensate Well Productivity using Capillary Number and Non-Darcy Effects", SPE 51910, Proceedings of the SPE Reservoir Simulation Symposium, (1999), Houston, TX.
9. Mott, R. E., Cable A. S., and Spearing, M. C., " Measurements of Relative Permeabilities for Calculating Gas-Condensate Well Deliverability", SPE Reservoir Eval. & Eng., (2000) **3** (6), 473.
10. Gravier, J. et al, "Determination of Condensate Relative Permeability on Whole Cores Under Reservoir Conditions", SPE Formation Evaluation, (1986), 9.
11. Henderson, G. D. et al, "Measurement and Correlation of Gas-Condensate Relative Permeability by the Steady State Method", SPEJ, (1996), 191.
12. Chen, H. L., Wilson, S. D. and Monger-McClure, T. G., "Determination of Relative Permeability and Recovery for North Sea Gas-Condensate Reservoirs", SPE Reservoir Eval. & Eng., (1999) **2,** 4, 393.
13. Whitson, C. H., Fevang, O., and Saevareid, A., "Gas Condensate Relative Permeability for Well Calculations", SPE 56476, SPE Annual Technical Conference and Exhibition, (1999) Houston, TX.
14. Huppler, J. D., "Water Flood Relative Permeabilities in Composite Cores", JPT, (1969), 539.
15. Ayyalasomayajulu, P. et al, "Measurement of Relevant Gas Condensate Relative permeability Data for Well Deliverability Predictions for a Deep Marine Sandstone Reservoir", SCA 2003-33, Intl. Symposium of the Society of Core Analysts, (2003), Pau, France.

Table 1. Composition and Properties of Model Fluids Used in the Study

Model Fluid	Components	Composition (mole %)		Pressure (psia)	Temperature (Deg. F)	Max. Liquid Dropout (%)	IFT (dynes/cm)
Binary		L	V				
Hydrocarbon	C_1	58.0	84.1	1710	100		0.59
Mixture	n-C_4	42.0	15.9				
Ternary	C_1	72.6		1750	175	30	0.98
Hydrocarbon	n-C_4	24.4					
Mixture	n-C_{10}	3.0					
Ternary	n-C_7	7.7		Ambient	Ambient		0.60
Aqueous	Brine	62.4					
Mixture	Isopropyl Alcohol	29.9					

Table 2. The Lean and Rich Gas Condensate Composition

Component	Composition (Mole %)		Component	Composition (Mole %)		Component	Composition (Mole %)	
	Lean	Rich		Lean	Rich		Lean	Rich
Nitrogen	0.09	1.07	Propane	2.34	4.77	n-Pentane	0.33	0.79
CO_2	4.23	0.71	i- Butane	0.34	0.80	C_6	0.42	1.00
Methane	82.32	70.91	n-Butane	0.83	1.73	C_{7+}	3.29	8.68
Ethane	5.54	8.98	i-Pentane	0.27	0.56			
IFT (dy/cm)	0.6	0.5	Gas Vis.(cp)	0.03	0.03	Liq. Vis.(cp)	0.23	0.12

Table 3. Properties of Sandstone Core Plugs and Core Composites

Core Composite	Plug Number	Porosity (% BV)	Permeability to Gas (mD)	Swi %	Permeablity at S_{wi} (mD)
A	1	8.8	33.6	9.2	30.2
	2	4.1	39.1		
	3	3.5	30.5		
	4	9.7	20.9		
B	1	15.1	57.1	0.0, 22.9	23.1, 13.9
	2	16.6	69.5		
	3	7.5	30.8		
	4	13.8	38.5		
C	1	18.9	4.4	25.2	1.5
	2	18.6	0.5		
	3	10.5	3.9		
	4	16.2	2.9		
	5	12.1	0.8		
	6	20.9	1.6		
D	1	17.1	8.1	0.0, 28.0	7.8, 7.3
	2	18.8	8.4		
	3	16.1	7.2		
	4	15.2	7.0		
E	1	11.1	3.7	35.2	2.1
	2	14.0	2.6		
	3	10.6	2.7		
	4	13.1	2.7		

Table 4. Properties of Carbonate Core Plugs and Core Composites

Core Composite	Plug Number	Porosity (% BV)	Permeability to Gas (mD)	Swi %	Permeablity at Swi (mD)
F Cordova Cream Limestone	1 2 3 4	23.5 24.2 20.2 26.1	10.1 4.0 5.6 4.8	0.0, 15.0	5.5, 4.0
G Carbonate Lagoonal	SinglePlug 4" long	13.1	20.0	15.9	11.2
H Carbonate Reef	Single Plug 4" long	17.0	21.3	13.6	7.6

Table 5. Flow Test Matrix (X Indicates Test Performed at Specified S_{wi})

Core →		SandStone					Carbonates		
Fluid System ↓		A	B	C	D	E	Cordova Cream Limestone	Carbonate Lagoon	Carbonate Reef
		← Composites of 4 to 6 plugs →						← Single Plugs →	
Model Fluids	Binary Liquid-Vapor				X S_{wi} = 28%				
	Ternary 1 Hydrocarbon							X S_{wi} = 15.9%	X S_{wi} = 13.6%
	Ternary 2 Aqueous	X S_{wi} = 0%	X S_{wi} = 0%	X S_{wi} = 0%	X S_{wi} = 0%		X S_{wi} = 15%		
Reesrvoir Fluids	Lean Gas-Condensate	X S_{wi} = 9.2%	X S_{wi} = 0, 22.9%	X S_{wi} = 25.2%			X S_{wi} = 0%		
	Rich Gas-Condensate				X S_{wi} = 0, 26.5 %	X (S_{wi} = 35.2%)			

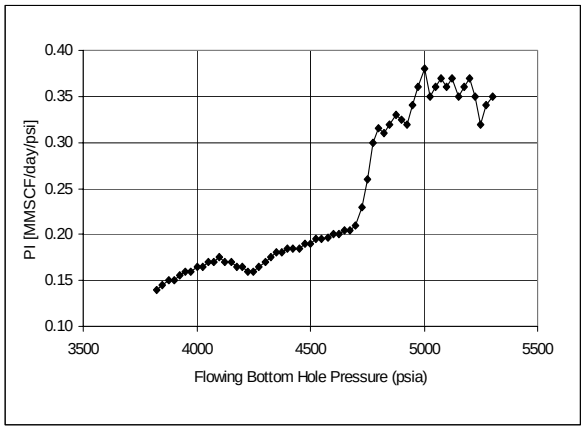

Figure 1. Productivity Index (PI) as a Function Flowing Bottom Hole Pressure (Lean Condensate Well)

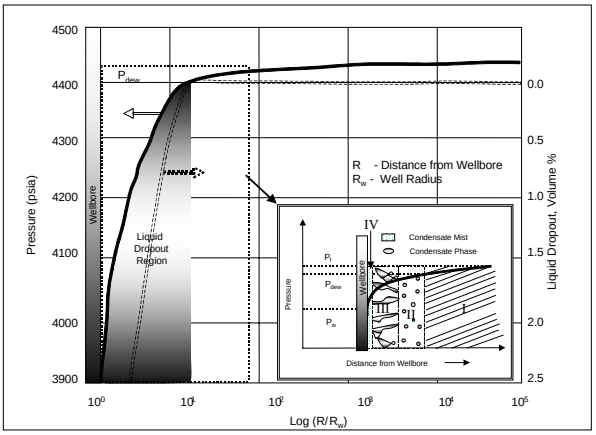

Figure 2. Liquid Dropout, Pressure Profile, and Flow Regimes in a Gas-Condensate Reservoir

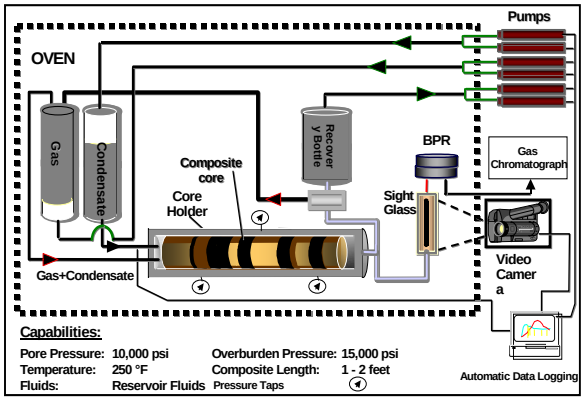

Figure 3. Schematic of Reservoir-Condition Apparatus

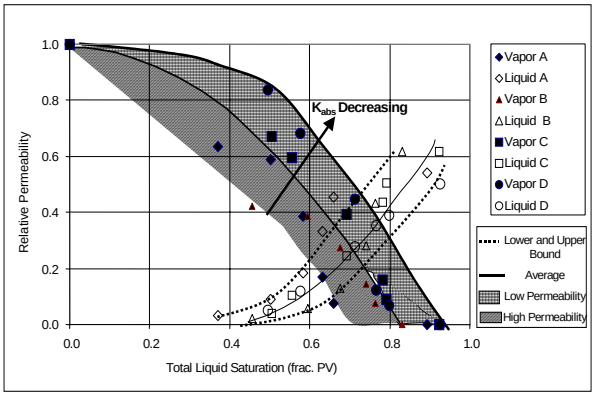

Figure 4. Ternary Liquid-Liquid Relative Permeability (Sandstones)

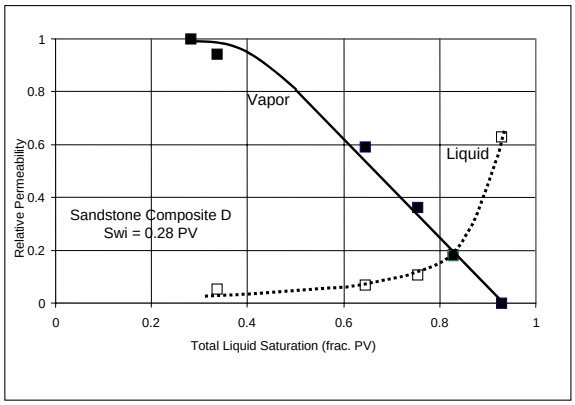

Figure 5. Binary Model Fluid Relative Permeability

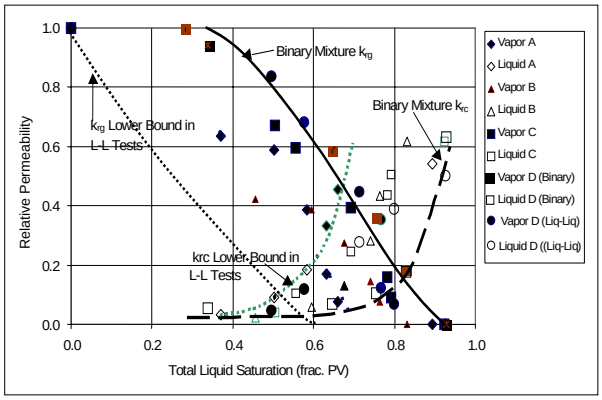

Figure 6. Model Fluid Relative Permeability Comparison - Sandstone Composites

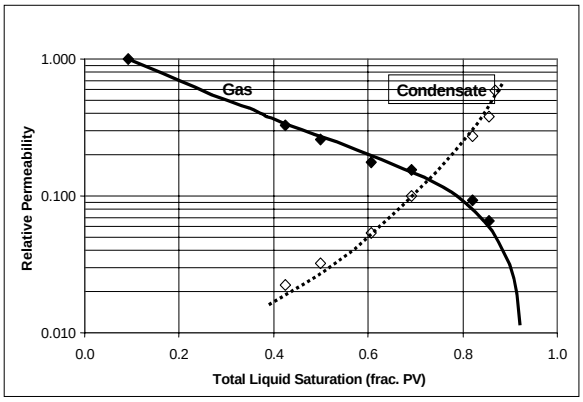

Figure 7. Lean Gas-Condensate Relative Permeability at Reservoir Condition
Sandstone Composite A (S_{wi} = 9.2%)

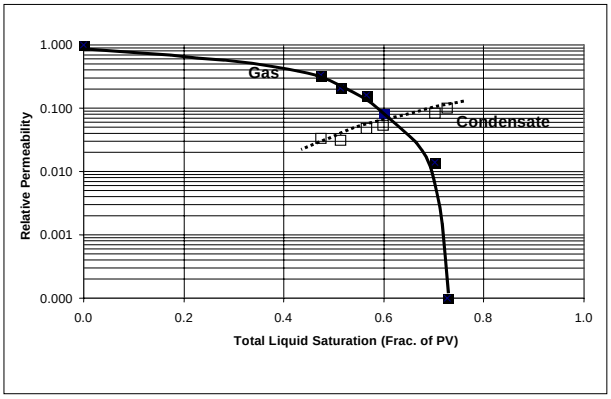

Figure 8. Rich Gas-Condensate Relative Permeability at Reservoir Conditions
Sandstone Composite D (S_{wi}=0%)

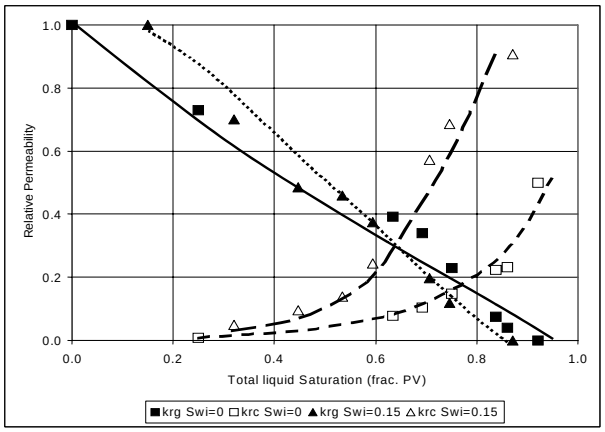

Figure 9. Liquid-Liquid Model Fluid Relative Permeability
Cordova Cream Limestone At S_{wi} = 0.0 and 0.15

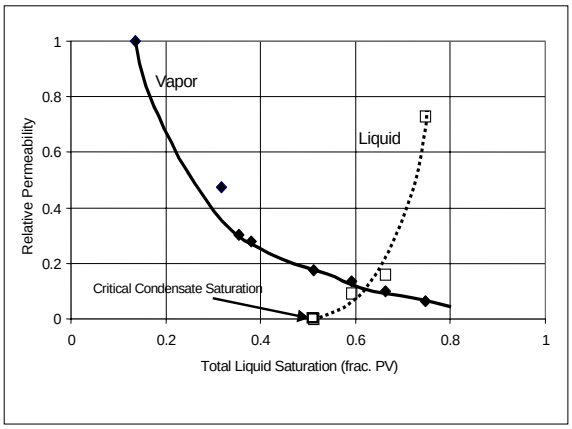

Figure 10. Ternary Hydrocarbon Model Fluid Relative Permeability
Carbonate Reef At S_{wi} = 0.136

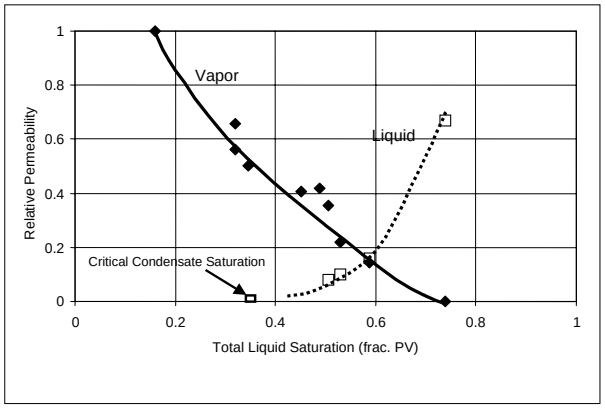

Figure 11. Ternary Hydrocarbon Model Fluid Relative Permeability
Carbonate Lagoonal At S_{wi} = 0.136

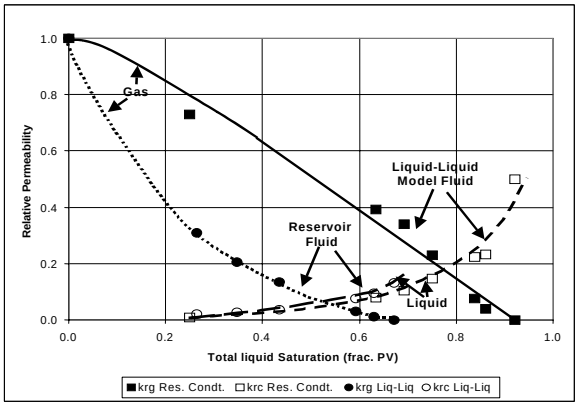

Figure 12. Relative Permeability Comparison
Reservoir Fluid vs. Model Fluids-Cordova Cream Limestone at S_{wi} = 0.0%

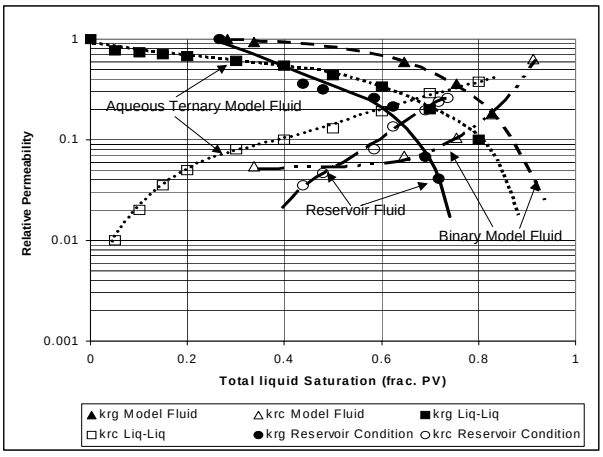

Figure 13. Relative Permeability Comparison
Actual Reservoir Fluid (Rich Condensate) vs. Model Fluids - Sandstone Composite

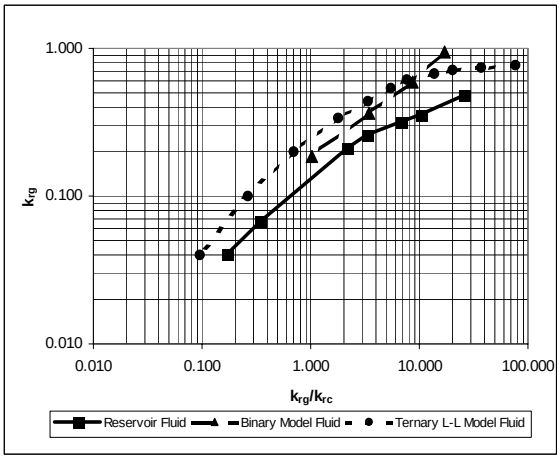

Figure 14. Relative Permeability Comparison
Reservoir Fluid (Rich Condensate vs. Model Fluids - Sandstone Composite D

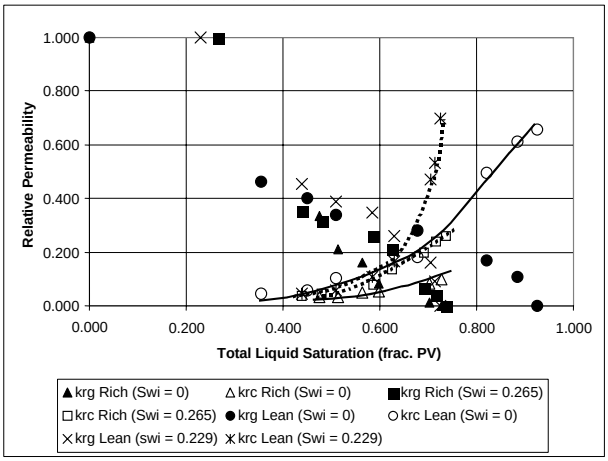

Figure 15. Effect of Initial Water Saturation on Relative Permeability
Reservoir Fluid Tests